THE JOURNAL OF PHYSICAL CHEMISTRY B
A JOURNAL OF THE AMERICAN CHEMICAL SOCIETY

pubs.acs.org/JPCB

Article

Combined NMR and UV−Vis Spectroscopic Studies of Models for the Hydrogen Bond System in the Active Site of Photoactive Yellow Protein: H-Bond Cooperativity and Medium Effects

Benjamin Koeppe,* Peter M. Tolstoy, Jing Guo, Gleb S. Denisov, and Hans-Heinrich Limbach

Cite This: https://doi.org/10.1021/acs.jpcb.0c09923

Read Online

ACCESS | Metrics & More | Article Recommendations | Supporting Information

ABSTRACT: Intramolecular hydrogen bonds in aprotic media were studied by combined (simultaneous) NMR and UV−vis spectroscopy. The species under investigation were anionic and featured single or coupled H-bonds between, for example, carboxylic groups and phenolic oxygen atoms $(COO\cdots H\cdots OC)^-$, among phenolic oxygen atoms $(CO\cdots H\cdots OC)^-$, and hydrogen bond chains between a carboxylic group and two phenolic oxygen atoms $(COO\cdots H\cdots(OC)\cdots H\cdots OC)^-$. The last anion may be regarded as a small molecule model for the hydrogen bond system in the active site of wild-type photoactive yellow protein (PYP) while the others mimic the corresponding H-bonds in site-selective mutants. Proton positions in isolated hydrogen bonds and hydrogen bond chains were assessed by calculations for vacuum conditions and spectroscopically for the two media, CD_2Cl_2 and the liquefied gas mixture $CDClF_2/CDF_3$ at low temperatures. NMR parameters allow for the estimation of time-averaged H-bond geometries, and optical spectra give additional information about geometry distributions. Comparison of the results from the various systems revealed the effects of the formation of hydrogen bond chains and changes of medium conditions on the geometry of individual H-bonds. In particular, the proton in a hydrogen bond to a carboxylic group shifts from the phenolic oxygen atom in the system $COO^-\cdots H-OC$ to the carboxylic group in $COO-H\cdots(OC)^-\cdots H-OC$ as a result of hydrogen bond formation to the additional phenolic donor. Increase in medium polarity may, however, induce the conversion of a structure of a type $COO-H\cdots(OC)^-\cdots H-OC$ to the type $COO^-\cdots H-(OC)\cdots H-OC$. Application of these results obtained from the model systems to PYP suggests that both cooperative effects within the hydrogen bond chain and a low-polarity protein environment are prerequisites for the stabilization of negative charge on the cofactor and hence for the spectral tuning of the photoreceptor.

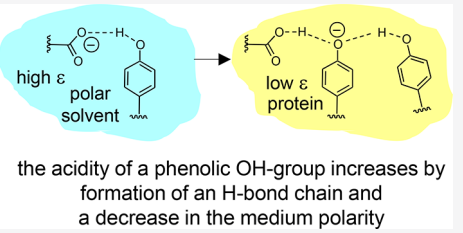

INTRODUCTION

Photoactive yellow protein (PYP, 14 kDa, 125 amino acid residues) is a photoreceptor related to a negative phototactic response of the purple bacterium *Ectothiorhodospira halophila*.[1,2] Upon irradiation, the protein undergoes a photocycle involving several states with characteristic UV−vis absorption spectra.[3] X-ray and neutron crystal structures of the protein in the dark state have been determined.[4,5] A schematic representation of the active site centered on the cofactor—a 4-hydroxycinnamic acid residue tethered to the side chain of Cys69 through a thioester linkage—is given in Figure 1a. Within the active site, which is a hydrophobic region of the protein, the phenolic oxygen atom of the cofactor takes part in a hydrogen bond system to the side-chain carboxylic group of Glu46 as well as to the phenolic oxygen atom of Tyr42 and the hydroxyl group of Thr50. According to Yamaguchi et al.,[5] the H-bond to Glu46 is almost linear, exhibits an O...O distance of 2.56 Å, and the bridging particle takes an almost central position less than 0.1 Å offset toward the carboxylic group (a "low barrier H-bond (LBHB)"). According to that model, the H-bond between the cofactor and Tyr42 is tendentially even shorter but nonlinear and much more asymmetric. The bond involving Thr50 bond is quite long (2.83 Å).[6] Altogether, the H-bond chain carries a negative charge that resides mainly on the cofactor[7]—this aspect is crucial for the spectral tuning[8] of the chromophore, which gives rise to blue light absorption (maximum at 446 nm) and thus to the characteristic color of the protein.[9] The negative charge in the active site is stable against protonation even in quite acidic solutions (apparent $pK_a = 2.7$).[6,10,11] Both this stability in acidic environments and the localization of the charge on the phenolic cofactor (instead of Glu46) are remarkable considering the pK_a values of isolated molecular fragments in aqueous solution, which are about 4 for the carboxylic group[12] and at least 9 for all other individual hydroxyl groups forming the H-bond chain.[13] Several attempts have been made to rationalize this phenomenon. For example, the proximity of a positively charged guanidinium group of the side chain of Arg52 has been invoked as an argument[4,14,15] but seriously challenged on several grounds.[5,6] The influence of the

Received: November 3, 2020
Revised: March 27, 2021

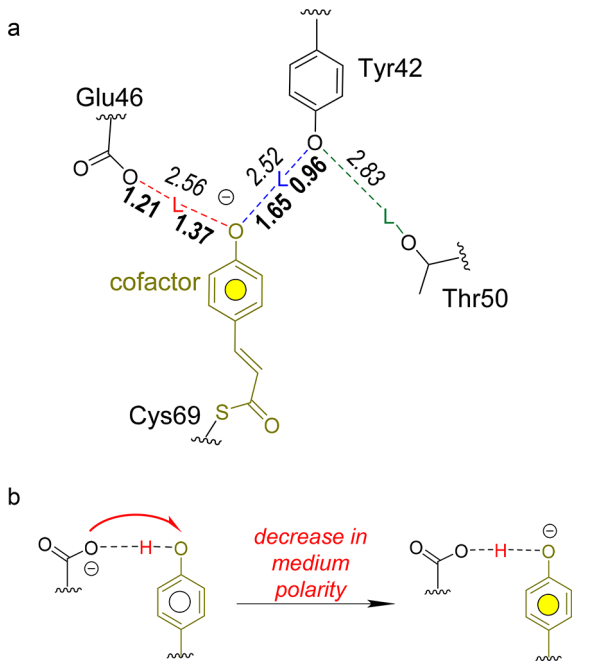

Figure 1. (a) Schematic representation of the hydrogen bonds in the active site of photoactive yellow protein in the dark state. Distances (in Å) of O−L bonds (in bold; L = light particle H or D) and O...O connectivities (in italics) are the result of a combined analysis of X-ray (L = H) and neutron diffraction data (L = D).[5] (b) In phenol carboxylate complexes, the decrease of medium polarity tendentially favors a transition from protonated (open circle) to deprotonated (yellow circle) phenolic moieties (split arrow indicates shift of electron density).[21]

active site hydrogen bond system on charge stabilization has been explored by studies of site-specific PYP mutants.[6,16] The species studied were lacking one of either the indirect (Thr50Val) or the direct (Tyr42Phe) hydrogen bond partners of the cofactor.[6] In the latter case, Thr50 took over the role of Tyr42 by forming a direct H-bond to the cofactor.[6] Both these mutants still undergo a photocycle in which the dark state absorbance maximum in both cases is red-shifted with respect to the wild-type protein—there hence is no evidence for a loss of the negative charge on the cofactor.[6] However, more recent studies of the Tyr42Phe mutant show that this species may under certain conditions adopt a blue-shifted dark state form in which the cofactor has evidently lost most of its negative charge:[17] the coexistence of both forms in macroscopic samples then gives rise to double peaks in UV−vis absorption spectra.

Coming back to the ground state of wild-type PYP, it should been noted that an alternative interpretation[18] for the neutron structural data of Yamaguchi et al. exists that in contrast to original authors' model (represented here by Figure 1a)[5] does not involve a particularly short and symmetric H-bond formed by Glu46. That more recent interpretation aligns much better with results from Sigala et al.,[41] who studied PYP by the liquid state ^{1}H NMR in aqueous solution and found signals at 15.2 and 13.7 ppm, which they attributed to the bridging protons in the hydrogen bonds between the cofactor and Glu46 and the cofactor and Tyr42, respectively.

Aims. We present here systematic model studies of isolated and coupled hydrogen bonds in small molecules in aprotic media. The molecules studied contain phenolic and carboxylic functional groups mimicking the cofactor and amino acid side chains interacting in the active site of the protein. Hydrogen bonds are characterized by spectroscopic methods. The aim is to reveal cooperativity effects within the hydrogen bond chains, that is, the mutual influence on hydrogen bond geometries and charge distribution. We do not attempt to reconstruct the details of the protein's active site in our models but instead try to reproduce the relevant hydrogen-bonding phenomena among the essential molecular fragments. The aprotic solvent models the hydrophobic environment of the active site which is shielded from the aqueous surroundings of the protein. It has been shown before that aprotic solvents, such as halogenated hydrocarbons, are a more suitable model for the interior of proteins than protic solvents such as water.[19] Particularly for the active site of PYP, computations predict a vital role of medium polarity on H-bond structure.[8,20] Experimentally, we have previously studied medium effects on phenol-carboxylate complexes in halomethanes and found that apolar conditions promote proton transfer from the phenol to the carboxylate and thus a shift of the charge to the former (Figure 1b).[21] Here, we aim to show that a combination of cooperativity and medium effects very well serves to explain the stabilization of the negative charge on the cofactor in dark state of PYP.

The species under investigation, compounds of the type **1**−**4**, are given in Figure 2. In these, the carboxylic, phenolic, and aliphatic hydroxyl groups interacting in the active site of PYP are covalently linked by methylene groups. **1** and **2** mimic the

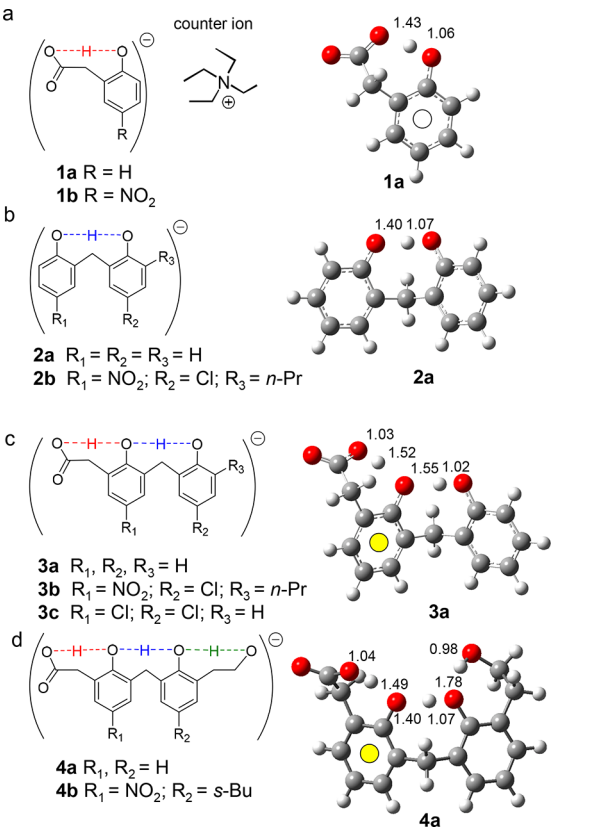

Figure 2. Left column: schematic structures (no specific H-bond geometries implied) and nomenclature of the species studied in this work. Right column: energy-optimized structures of anions **1a**−**4a** obtained in DFT calculations (B3LYP/6-311++G**, no medium, no counterions; distances in Å, open and yellow circles indicate protonation and deprotonation of phenolic residues, respectively).

https://doi.org/10.1021/acs.jpcb.0c09923
J. Phys. Chem. B XXXX, XXX, XXX−XXX

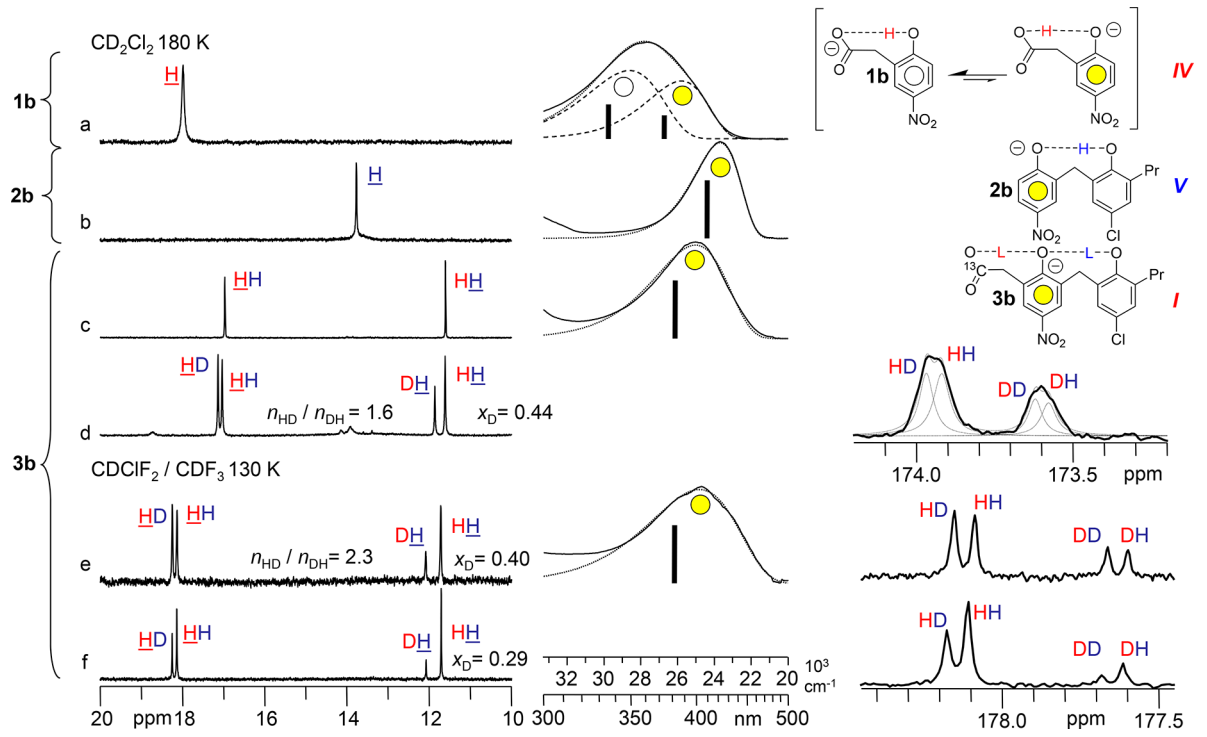

Figure 3. UV/NMR spectra of **1b** (a), **2b** (b), and **3b** (c–f). The latter were obtained at various total deuterium fractions (x_D = 0, 0.44, 0.40, and 0.29)[46] in the mobile proton sites. Spectra a–d were recorded in CD_2Cl_2 solution at 180 K; spectra e and f were recorded in $CDClF_2/CDF_3$ solution at 130 K. Dotted lines represent fit functions (log-normal and Lorentzian in optical and NMR spectra, respectively). Vertical bars in optical spectra represent centers of gravity and—where applicable—relative integral intensities of the fit functions. In the case of the coupled H-bonds of **3b**, two letters "LL" (light particle sites L = H or D) are used for signal attribution to isotopologues and their isotopomers: the order of mobile proton sites from left to right is the same as in the chemical structure (color coding as additional clarification); observed nuclei are underlined where applicable. Open and yellow circles highlight protonated and deprotonated moieties, respectively. Roman numbers classify H-bonds in terms of the proton transfer pathway depicted in Figure 4; in the case of **3b**, the H-bond to the carboxylic group is characterized.

individual hydrogen bonds between cofactor and side chains of Glu46 or Tyr42, respectively. Structures **3** model the pairs of coupled hydrogen bonds between Glu46 and the phenolic groups of the cofactor and Tyr42. Finally, in **4** there exists the additional possibility of formation of a third hydrogen bond to an aliphatic hydroxyl group (the side chain of Thr50). That third H-bond in this model is spatially limited to the nearest phenolic hydroxyl group representing Tyr42, even though we are aware that the literature also offers other options than the conventional structure according to Figure 1a, that is, H-bonding between Thr50 and the cofactor or the amide carbonyl of Glu46: by assuming a dynamic equilibrium among these structures, the group of Ochsenfeld[22] was the first to computationally explain the NMR signals of the bridging protons in the protein.

The choice of model systems **1**–**4** forming intramolecular hydrogen bonds was made after preliminary experiments had indicated that intermolecular associates of two phenol moieties with a carboxylate formed in aprotic solvents tend to adopt structures in which the carboxylic group takes the *central* position in the hydrogen bond chain. For modeling the PYP active site H-bond system, however, it is essential that the carboxylic group be in the *terminal* position.

Structures **1a** to **4a** were treated by gas-phase DFT calculations to assess the geometric feasibility of intramolecular hydrogen bond formation. Compounds **1b** to **4b** and **3c** were synthesized and studied spectroscopically. The choice of the substituents in these species followed various considerations concerning UV–vis spectroscopic properties, the proton-donating abilities of the protic groups of the respective subunits, or experimental aspects such as solubility. It might be argued that models involving a hydroxycinnamyl thioester would be desirable with respect to a close match to the cofactor chromophore. Unfortunately, such species are experimentally problematic because of their low solubility in halocarbons and their strong propensity toward hydrolysis by residual water in such media.[23] Instead, we used the 4-nitrophenyl moiety whose UV–vis spectroscopic properties in hydrogen-bonded complexes have been extensively studied: they display maxima in light absorbance between approximately 300 nm (near-UV) and 420 nm (blue light) depending on the protonation state, in a similar fashion as hydroxycinnamyl thioesters.[21,24] It is important to note that the other phenolic moieties (not bearing a nitro substituent) absorb light only at considerably shorter wavelengths; thus, the nitrophenolic residues can be monitored with sufficient spectral separation in models **1b**, **2b**, **3b**, and **4b**. 4-Nitrophenyl residues, however, have a pK_a of ca. 7 and are hence substantially more acidic than the hydroxycinnamyl thioester residue of the PYP cofactor (pK_a 9).[13] For the sake of a more accurate representation of the intrinsic proton-donating abilities of the groups interacting in PYP, we also consider species **3c** whose 4-chlorophenol fragments have an intrinsic pK_a of about 9.4.[25]

In the evaluation of NMR and UV–vis spectroscopic results, we apply spectroscopic hydrogen bond correlations to estimate positions of the bridging protons in the hydrogen bonds. Time-averaged hydrogen bond geometries may be assessed by

https://doi.org/10.1021/acs.jpcb.0c09923
J. Phys. Chem. B XXXX, XXX, XXX–XXX

NMR correlations,[26−29] most notably the resonance of the hydrogen-bonded proton itself that experiences deshielding on hydrogen bond formation and contraction.[30−33] H-bonds involving carboxylic groups may be assessed by ^{13}C chemical shifts and H/D isotope effects on that parameter.[28,34−39] An especially remarkable feature is the so-called "vicinal" H/D isotope effect on the shift of residual protons in partially deuterated hydrogen bond chains which may reveal the mutual interaction of individual H-bonds.[28,40−43]

Time-averaged geometric information from NMR will be complemented by results from optical spectroscopy with its much shorter characteristic time. In this context, two key results from a previous work[24] of some of us will be of central importance: a UV−vis spectroscopic hydrogen bond correlation and a proton transfer pathway involving tautomeric species (see the scheme in Figure 4 that will be extensively referred to within the Discussion section).

This paper is structured as follows. After the Experimental Section, a combined description of the results and their discussion will be given, beginning with the results on individual systems which is followed by a comparative discussion of all results and their implications with respect to the phenomena observed in PYP.

EXPERIMENTAL SECTION

DFT calculations, the syntheses of all model compounds, sample preparation, and spectroscopic experiments that make use of the previously introduced[44] and employed[21,24] setup for combined UVNMR spectroscopy are detailed in the Supporting Information.

RESULTS AND DISCUSSION

DFT Calculations. We optimized the geometries of the species given in Figure 2, left column (not including counterions or medium models): the monoanions of 2-hydroxyphenylacetic acid (**1a**, a "phenolic carboxylate") and bis(2-hydroxyphenyl)methane (**2a**, a "bisphenolate") as well as the monoanions **3a** (a "bisphenolic carboxylate") and **4a**. The resulting three-dimensional structures including O−H distances are shown in the right column of Figure 2. The O−H−O angles vary between 174° and 168°; C−O−H angles vary between 107° and 118°. O−H−O distances of <2.5 Å in **1a** and **2a** show that the molecules are capable of forming short and almost linear intramolecular hydrogen bonds. Both bonds in **3a** bear O−H−O distances of <2.6 Å. Thus, there are no signs of geometric constraints which might raise doubts concerning the generality of the results obtained from such models. Another interesting finding is that in **1a** the carboxylic group is deprotonated while in **3a** and **4a** these are protonated, and the adjacent phenolic units carry the charge (formally). We shall return to this aspect in the discussion of the experimental results.

NMR and UV−Vis Spectroscopic Results on 1b, 2b, and 3b. Spectra obtained from systems containing title species are given in Figure 3. All parameters of optical and NMR spectroscopy are collected in section 3.2 of the Supporting Information. All ^{1}H NMR spectra display signals corresponding to protons in hydrogen bonds which are relatively sharp (maximum line widths 35 Hz). Moreover, these signals (and only these) can also be observed at significantly higher temperatures (up to 250 K, not shown). This finding is in contrast to our previous observations in studies of intermolecular anionic complexes of carboxylic acid and phenols[21,24] in which the slow exchange regime for the signal of the bridging proton was usually reached only at temperatures below 200 K (samples were prepared by the same as the present techniques). We thus conclude that all signals in the spectra of Figure 3 are due to intramolecular H-bonds exclusively.

Specifically, the phenolic carboxylate **1b** (Figure 3a) exhibits a single proton resonance in the displayed part of the spectrum (18.1 ppm) and a broad optical absorption band ($\Delta\tilde{\nu}$ = 6200 cm^{-1}). Interestingly, very similar results have previously been obtained[21] for an intermolecular complex between 4-nitrophenol and 4-phenylbutyrate in CD_2Cl_2 (Figure S7 gives a direct comparison of these particular results in traces b and c as well as other comparative data). It had been concluded for the intermolecular complex that it may be pictured as existing in two tautomeric forms (both exhibiting strong H-bonds) of which the one that bears the bridging proton on the phenolic oxygen atom is more abundant—in the same fashion as we thus depict **1b** in Figure 3, top right. Following the approach that has been successfully employed in the analysis of UV−vis spectra of nitrophenols in intermolecularly H-bonded species,[21,24] we approximate the distribution of H-bond geometries in terms of an equilibrium between two tautomeric forms and attempt a deconvolution of the experimental spectrum into two components of log-normal shape[45] in the wavenumber dimension (skewness parameter 1.5). The results are visualized in Figure 3a: dashed lines give individual components and their sum; vertical bars indicate centers of gravity and relative integral intensities of the components (numerical values in Table S3). The fit is very satisfactory. We may now categorize system **1b** within the schematic proton transfer pathway depicted in Figure 4 (adapted from ref 21).

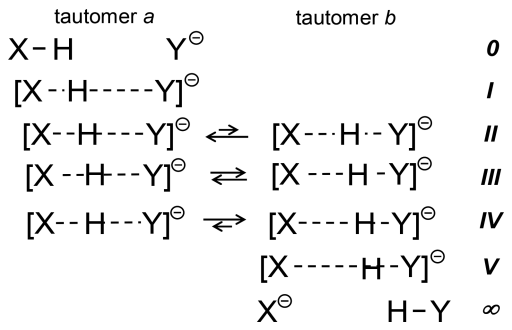

Figure 4. Schematic proton transfer pathway between XH and Y^- eventually leading to X^- and HY passing through tautomeric structures (*II* to *IV*) with very strong H-bonds (adapted from ref 21).

On the way between XH and Y^- to X^- and HY (where in the current case X^- and Y^- correspond to the carboxylate and phenolate fragments, respectively) **1b** is in stage *IV*. **1b** will serve as a reference in the analysis of the other systems.

Bisphenolate **2b** (Figure 3b) gives rise to proton resonance at 13.8 ppm and a UV−vis absorption band that is both significantly narrower and substantially red-shifted with respect to that of **1b**. The relatively strong shielding of the bridging proton is indicative of a rather long H-bond. The absorption maximum in the visible range is characteristic for 4-nitrophenol moieties carrying negative charge (see Figure S7 for a comparison). We therefore infer that the bridging proton in **2b** resides on the phenolic oxygen atom of the chloro-

https://doi.org/10.1021/acs.jpcb.0c09923
J. Phys. Chem. B XXXX, XXX, XXX−XXX

substituted ring. The narrowness of the absorption band indicates that this is the only relevant structure existing in solution under the given conditions. According to Figure 4, we have a stage ***V*** proton transfer in this case (if one considers the nitrophenolic fragment donor XH).

Let us now focus our attention on the spectra of the dichloromethane solution of bisphenolic carboxylate **3b** (Figure 3c). In the ^{1}H NMR spectrum, there are two signals of equal integral intensity at 17.0 and 11.6 ppm. The UV−vis spectrum features a rather symmetric absorption band with a maximum at around 400 nm. This band is blue-shifted and broadened in comparison to that of the bisphenolate **2b** but red-shifted in comparison to the low-energy component of the phenolic carboxylate **1b** and not much broader than the latter. A short wavelength component at 350 nm and below is absent in **3b**. This suggests that within the H-bond chain of **3b** negative charge resides mostly on the nitrophenolic fragment, and the bridging protons reside exclusively on the terminal oxygen atoms of the H-bond chain as depicted in the schematic structure in Figure 3c. This means that the H-bond of the carboxylic group (XH) is in stage ***I*** of the proton transfer pathway (Figure 4)—a remarkable contrast to the stage ***IV*** found in **1b**. This shift is a central finding of this work to which we shall return to later.

The localization of the bridging particles in **3b** on the terminal oxygen atoms of the H-bond chain is further supported by the vicinal H/D isotope effects[28,40−42] evident in the proton spectrum in Figure 3d obtained from dichloromethane solution of **3b** partially deuterated in mobile proton sites. To simplify the discussion, we state at this point that—as will be verified later—the more deshielded proton HH is in the H-bond to the carboxylic group and HH is linking the phenolic oxygen atoms (left proton in the schematic structure of **3b** gives rise to the left signal in the proton spectrum). The two partially deuterated isotopomers HD and DH each give rise to signals at slightly lower field than the respective signals of the all-protonated isotopologues. This means that we are observing vicinal isotope effects $\Delta\delta$ within a chain of two coupled H-bonds, positive in terms of a definition $\Delta\delta = \delta_{\underline{H}D} - \delta_{\underline{H}H}$. This sign of the isotope effect is indicative of anticooperatively coupled H-bonds and a structure O−L···O^{-}···L−O in which the bridging particles L (H or D) reside on the *terminal* acceptor atoms of the hydrogen bond chain (a detailed description of an analogous case is given for example in Chart 4 of ref 28).

We note that the two isotopomers HD and DH of the singly deuterated isotopologue are *not* equally abundant; the equilibrium constant for the H/D exchange among the mobile particle sites

$$\mathrm{ODOHO} \overset{K_{HD}}{\rightleftharpoons} \mathrm{OHODO}$$

is K_{HD} = 1.7 (estimated from signal integration).[46] The isotopomer with the deuteron in the longer H-bond is more stable; that is, we observe the phenomenon of isotope fractionation.[47] All data in this context (integral signal intensities, deuteron fractions, and fractionation factors) are collected in Tables S7−S9.

Figures 3e and 3f give spectra of partially deuterated bisphenolic carboxylate **3b** in $CDClF_2/CDF_3$ solution recorded at 130 K; in the latter case, the deuterium fraction had been reduced by addition of sample solution with natural isotope abundance. The observed changes in signal intensities hence allow for the attribution of signals to fully protonated and partially deuterated species. The order, that is, increased shielding in the sequence HD > HH ≫ DH > HH, remains the same as in CD_2Cl_2 solution. From this follows that positive vicinal isotope effects and therefore anticooperative coupling within the H-bond chain are retained. The thus-implied location of the bridging particles on the terminal acceptor atoms of the hydrogen bond chain is further confirmed by the similarity of the optical spectra of **3b** obtained in the two solvents. The (apparent) broadening of the absorption band in $CDClF_2/CDF_3$ relative to CD_2Cl_2 solution is most likely an artifact caused by the inferior optical properties of the round bottomed (standard medium wall) NMR tube required for the former experiment.[48]

Returning to the proton NMR spectra of **3b** in $CDClF_2/CDF_3$, we note that the intensity ratio of signals HD and DH in this case corresponds to K_{HD} = 2.3. This reflects the increase in difference in hydrogen bond lengths (in comparison to the CD_2Cl_2 medium with K_{HD} = 1.7) and the increase in disparity of vibrational potentials in the two mobile particle sites. The analyses of signal intensities in the proton spectra in Figure 3e,f also allow us to estimate the deuterium fractions x_D in the samples,[46] namely 0.40 and 0.29. These, and the isotope fractionation, will help us to establish the signal attribution in the ^{13}C NMR spectra of the corresponding samples (far right of Figure 3e,f). The spectral region corresponds to carboxylic carbon signals of **3b**, which was ^{13}C enriched in that position.

First, the most and least intense signals at low deuterium fraction (Figure 3f) are caused by the fully protonated and fully deuterated isotopologues HH and DD, respectively. The signals of the two remaining species HD and DH are then readily identified considering their 2.3:1 molar ratio estimated from the ^{1}H NMR spectrum.

Let us assess the H/D isotope effects in the ^{13}C NMR spectrum: there are a large negative $\delta(\mathrm{DH}) - \delta(\mathrm{HH}) = -0.49$ ppm and a small positive isotope effect $\delta(\mathrm{HD}) - \delta(\mathrm{HH}) = +0.06$ ppm. It has been well established[36] that the large negative isotope effect indicates a *short* hydrogen bond in which the bridging particle is located on the carboxylic group. This confirms the qualitative placement of the bridging particles in **3b** made above on grounds of ^{1}H NMR and UV−vis results, and it also verifies the assumption (introduced above as a plain statement) that the bond to the carboxylic group is the significantly shorter of the two H-bonds in **3b**. A reasoning for the latter that is not depending on conclusions drawn from previous work with intermolecular complexes[36] goes as follows. The large isotope effect on the resonance of the carboxylic group must be caused by deuteration of a bond the carboxylic group is directly involved in (not by an even more indirect effect). The carbon spectrum of Figure 3e immediately shows that this large effect is observed in the *less* populated isotopomer of the semideuterated isotopologue (signal at 177.6 ppm).[49] The less populated isotopomer, however, must be the one with the deuteron in the short H-bond (bearing a wide potential curve);[47] thus, the H-bond to the carboxylic group must be the shorter of the two.

The ^{13}C NMR spectrum of partially deuterated **3b** in CD_2Cl_2 solution (far right of Figure 3d) which we did not address yet is readily interpreted in analogy to what has been found for the same complex in the other medium: in terms of two pairs of signals where the small splitting is not quite resolved (Lorentzian least-squares fit is given as broken lines). We note that the isotope effect $\delta(\mathrm{DH}) - \delta(\mathrm{HH}) = -0.34$ ppm

https://doi.org/10.1021/acs.jpcb.0c09923
J. Phys. Chem. B XXXX, XXX, XXX−XXX

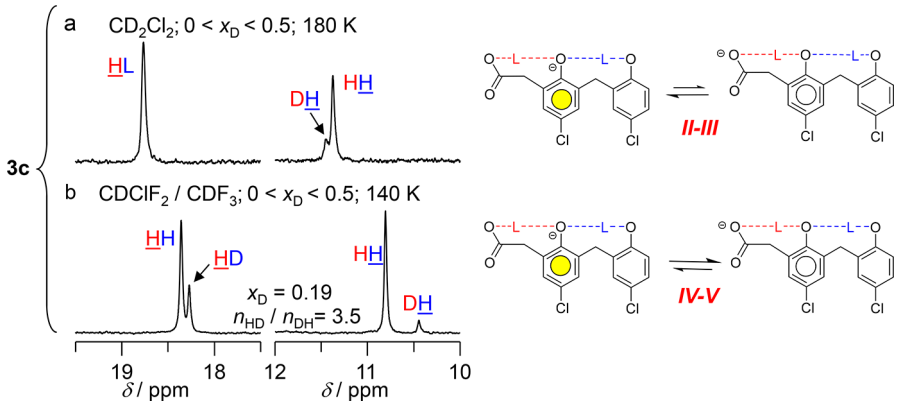

Figure 5. ^{1}H NMR spectra of the dichlorobisphenolic carboxylate **3c** partially deuterated in the mobile proton sites: (a) in CD_2Cl_2 solution at 180 K; (b) in $CDClF_2/CDF_3$ solution at 140 K. Conventions are analogous to those introduced in the caption of Figure 3. Schematic structures given are results of the analysis given in the main text.

is reduced in this solvent with respect to $CDClF_2/CDF_3$. This coincides nicely[36] with a lengthening of the shorter of the two H-bonds that is evidenced by the proton spectra. In contrast, the geometry of the longer H-bond is hardly medium dependent. This is further evidence in line with the arguments laid out in the previous paragraph.

NMR Spectroscopic Results on 3c. Selected regions of the ^{1}H NMR spectra of the dichlorobisphenolic carboxylate **3c** with a small deuterium fraction in the mobile proton sites are shown in Figure 5. We will first focus our attention on Figure 5b corresponding to a $CDClF_2/CDF_3$ solution at 140 K. The two major signals that are of equal integral intensity we attribute to the nondeuterated species HH. The two minor of the four signals, labeled HD and DH, correspond to partially deuterated species in a molar ratio of 3.4:1, respectively. Thus, in contrast to the situation in the nitro derivative **3b**, we in this case see *negative* vicinal isotope effects corresponding to a chain of cooperatively coupled hydrogen bonds of the schematic structure $O^-\cdots L-O\cdots L-O$. Signal attribution otherwise is analogous to that in the case of **3b**: HL and LH are the bridging protons in the short hydrogen bond to the carboxylic group and the considerably longer bond between phenolic oxygen atoms, respectively. The H-bond of the carboxylic group could be of in stage ***IV*** (two tautomers) or in stage ***V*** (single tautomer). In the absence of suitable UV−vis data, no safe distinction is possible. However, stage ***IV*** seems more likely: in ref 24, only tautomeric structures (stages ***II*** to ***IV***) have been found for isolated intermolecular phenol-carboxylate H-bonds displaying proton chemical shifts >18 ppm.

Moving on to CD_2Cl_2 solution spectra of dichlorobisphenolic carboxylate **3c**, we direct our attention to Figure 5a (partially deuterated sample, recorded at 180 K). In this medium, only three signals appear, of which the weakest (at 11.45 ppm) is just resolved from the neighboring one at 11.37 ppm and attributable to the partially deuterated isotopologue. The proton in the shortest hydrogen bond is strongly deshielded (rather broad signal at 18.8 ppm).

Hence, in contrast to the previous situation in the Freonic medium, we observe a *positive* vicinal isotope effect on the signal of the proton in the longer hydrogen bond (HH, DH), that is, anticooperatively coupled bonds and localization of the briging particle LL on the carboxylic group.

However, no vicinal isotope effect is observable for the signal of the proton in the short hydrogen bond (HL). Altogether, this gives clear evidence for a tautomeric equilibrium in which all signals (and isotope effects) are weighted time averages. The barely resolved *positive* vicinal isotope effect indicates that we have a carboxylic group H-bond in stage ***II*** to ***III***; that is, the dominance of the tautomer with the protonated carboxylic group is so small that the (intrinsically small) vicinal isotope effects induced by the longer H-bond average beyond resolution, i.e., to a single rather broad HL signal instead of separate signals HH and HD.

NMR Spectroscopic Results of 4b. Figure 6 shows ^{1}H NMR spectra of our most extended model **4b** in CD_2Cl_2 (a, b) and Freon solutions (b, c), of which the latter in each case were obtained from samples partially deuterated in the mobile proton sites.

At first glance, results look quite similar to those on the simpler analogue **3b**. There are no additional signals in the spectra (including those regions omitted in Figure 6) which we could readily attribute to a third hydrogen bond. It clearly is the aliphatic hydroxyl group for which we expect the longest and weakest of the three possible H-bonds. Thus, in analogy to **3b**, we attribute the signals as shown in Figure 6, top right, that is, to an anticooperatively coupled pair of H-bonds to the carboxylic group and the two phenolic oxygen atoms. Any signal(s) of the aliphatic hydroxyl group could easily be obscured by exchange-related broadening and the other signals in the high-field part of the spectrum (not shown). Nonetheless, the line shape analyses of the 12−12.9 ppm regions of the spectra in Figure 6c,d given in the inset reveals evidence for an H-bond involving the aliphatic hydroxyl group. We first observe that already in the absence of deuteration (top of inset) the signal attributed to HHH displays a minor doublet splitting of 0.045 ppm (again, throughout this paper, specifications such as HHH always follow the left-to-right order in the chemical structures; color coding is only additional support, i.e., here we are referring to the H-bond between the phenolic oxygen atoms). Within this work, such a phenomenon of signal splitting of unclear reason has been observed exclusively (and reproducibly) in the *sec*-butyl-containing **4b** and is likely due to diasteriomeric structures.[51] More importantly, however, analysis of the line shape in the case of partial deuteration (bottom of inset) reveals yet *two* more splittings on top of the diasteriomeric differentiation—instead of just one vicinal isotope effect from the H-bond to the carboxylic group. The smaller of the two splittings (by chance again 0.045 ppm) is very likely to originate from the

https://doi.org/10.1021/acs.jpcb.0c09923
J. Phys. Chem. B XXXX, XXX, XXX−XXX

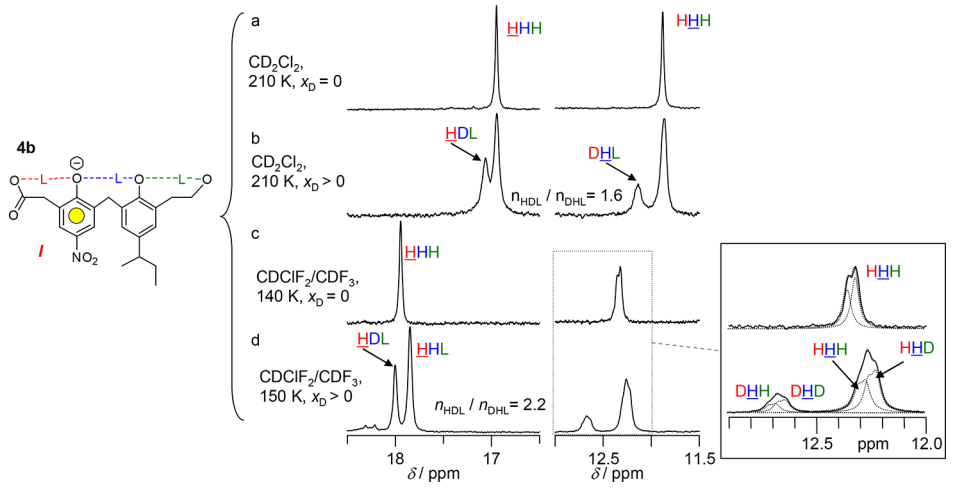

Figure 6. ^{1}H NMR spectra of the TEA salt of **4b**. Solvents, temperatures, and deuteration ratios were varied as individually specified. Conventions are analogous to those introduced in the caption of Figure 3: codes like HDL designate light particle sites from left to right as in the chemical structures; thus, in this example it refers to the signal of a carboxylic proton that is next to a central deuteron which is followed by any nucleus in the last H-bond (no individual signals for HDH and HDD are resolved). In (d), the estimated site specific deuterium fractions[50] are x_{DLL} = 0.22, x_{LDL} = 0.37, and x_{LLD} = 0.56 at a total deuterium fraction of 0.39.

additional H-bond to the aliphatic hydroxyl group: that is, besides HHH we also observe DHH, DHD, and HHD. The bond formed by the observed proton is cooperatively coupled to the additional bond in question. Analysis of signal intensities leads to the following deuterium fractions in the three mobile proton sites: x_{DLL} = 0.22, x_{LDL} = 0.37, and x_{LLD} = 0.56.[50] This means that we have access to isotope fractionation information for (and thus to a characteristic parameter of)[47] the long H-bond to the aliphatic hydroxyl group even though we cannot identify the signal of its bridging proton in the spectrum.

We conclude that in **4b** a chain of three coupled intramolecular hydrogen bonds is formed. The rather long hydrogen bond formed by the aliphatic hydroxyl group has only little (but measurable) influence on the other two hydrogen bonds in the chain. Findings for the latter part of the H-bond chain are therefore quite similar to those in the simpler analogue **3b**.

Model Results and Photoactive Yellow Protein. Let us summarize the observations on the proton positions in the intramolecular hydrogen bonds within the model anions that we studied.

We have a short tautomeric hydrogen bond in the phenolic carboxylate **1b** (Figure 3a) and the bridging proton resides predominantly on the phenolic oxygen atom (proton transfer stage ***IV***). In the bisphenolate **2b** (Figure 3b) there is a longer hydrogen bond, and the bridging proton is located exclusively on the chloro-substituted ring (no tautomerism, proton transfer stage ***V***). In the bisphenolic carboxylate **3b** (Figure 3c), which combines both types of hydrogen bonds present in **1b** and **2b**, a structure of the type O−H···O^{-}···H−O is formed in which the proton resides exclusively on the carboxylic group (proton transfer stage ***I***), leaving the negative charge on the central phenolic acceptor.

This is a key finding of this work for which the analogue was observed in gas phase calculations: in the phenolic carboxylate **1a** (Figure 2a) the bridging proton is located on the phenolic oxygen atom, and negative charge is on the carboxylate group; but in the bisphenolic carboxylates **3a** and **4a** (Figures 2c and 2d) one of the bridging protons is located on the carboxylic group, and the central phenolic acceptor bears the negative charge.

Figure 7 summarizes the rationalization for all these observations: formation of the phenol−phenol H-bond (and thus the H-bond chain) shifts electron density toward the terminal phenol (arrow 1a) and—as a secondary effect mediated by an opposite shift of the other bridging proton—away from the carboxylic group (arrow 1b). Eventually, charge may be formally located on the central phenolic moiety where it is "chelated" by two bridging protons that, however, both predominantly reside on the the terminal H-bond donors. The very same phenomenon should be effective in the dark state of PYP: the cofactor's hydrogen bond to Tyr42 promotes proton transfer between the cofactor and the side chain carboxylic group of Glu46; the cofactor becomes negatively charged and thus tuned to blue light absorption.

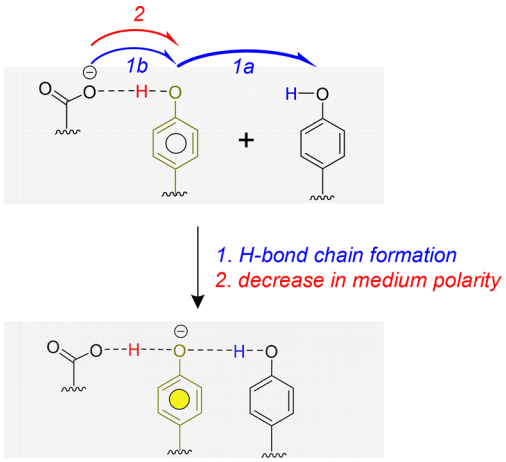

Figure 7. Schematic summary of the effects promoting deprotonation of the central phenol moiety in the PYP-type H-bond chain as described in the text. Half arrows indicate shifts of electron density; open and yellow circles highlight protonated and deprotonated moieties, respectively.

https://doi.org/10.1021/acs.jpcb.0c09923
J. Phys. Chem. B XXXX, XXX, XXX−XXX

Charge transfer away from the carboxylic group is further aided by low−medium polarity (arrow 2 in Figure 7).[21] In model **3b**, the negative charge is located on the central phenolic unit in a relatively low polarity solvent (CD_2Cl_2 at 180 K exhibits $\varepsilon \approx 18$)[52] as well as under more polar conditions ($CDClF_2/CDF_3$ at 130 K with $\varepsilon \approx 30$).[53] In **3c**, however, in which intrinsic acidities of hydrogen bond donors more closely resemble those of the groups interacting in the protein, the negative charge on the phenol ring is barely stabilized in CD_2Cl_2 solution and clearly shifts toward the carboxylic group when medium polarity is increased. Moreover, DFT calculations on **3a** suggest that in the absence of a medium the phenol ring takes the charge even if electron-withdrawing substituents such as chlorine atoms and nitro groups are absent. Taken together, these findings confirm those on the medium effect on phenol-carboxylate hydrogen bonds in halomethanes experimentally demonstrated for intermolecular complexes previously[21] and agree with the computational results laid out in refs 8 and 20—despite the lack of an obvious trend in a more heterogeneous set of media of different polarity reported intermittently.[54]

Comparison of models **3b** and **4b** shows that the hydrogen bond in **4b** formed by the aliphatic hydroxyl group mimicking the side chain of Thr50 is rather long and has little impact on the remainder of the hydrogen bond chain. Further comparison of our results from models **3b** and **3c** with those for PYP by Sigala et al.[41] reveals that in the protein the H-bonds of the carboxylic groups and the ones between the phenolic oxygen atoms are lengthened and shortened, respectively, relative to their equivalents in our models. The common trend in these changes is a shift of the bridging particles toward the carboxylic group when regarding the situation in the protein as the reference. Considering again the medium effect on phenol carboxylate complexes illustrated by Figure 1b,[21] we would expect a *reduction* in solvent polarity to change H-bond geometries within the model anions in that sense and provide a closer match with the situation in the protein. Such an optimization could lead to an experimental estimation of an "effective medium polarity" of the protein environment which—considering the given trend—we expect to be quite low.[55] Unfortunately, in practice, this approach is difficult to realize with the current model anions due to their insufficient solubility in apolar media.

Even though there is evidence in the current case that the environment of the COO···H···(OC) hydrogen bond of the PYP active site is best modeled by a rather apolar medium, we would like to point out that caution should be exhibited in attempts of extrapolating this result to other systems. It was shown for example in a work on hydrogen bonds in the active site of aspartate aminotransferase that in that case an aprotic solvent with dielectric constant of 30−40 is an appropriate model medium.[19] Moreover, one should always bear in mind that when speaking about interior of a protein the term "polarity of the medium" refers to local electric fields and does not have the same meaning as the dielectric properties of a polarizable continuum or an organic solvent. In a polar aprotic solvent, the hydrogen bond geometry is influenced by the intermolecular interactions with the surrounding solvent molecules. The latter relax around the solute and create the reaction electric field which may lead to significant displacement of the bridging particle as compared to the same complex in a vacuum. Sometimes it is worth to describe this phenomenon by using such macroscopic parameter as dielectric constant of the medium. This description is a gross model attempting to summarize all the effects of solvent−solute interactions in a single parameter. When talking about H-bond geometry in aprotic solution, a single value of the dielectric constant ε substitutes the phrase "due to the intermolecular interactions the hydrogen bond geometry changes upon solvation are such as if the complex is affected by the reaction field of a polarizable continuum with dielectric constant ε". The more details of the environment are described explicitly—as for example, in MD simulations[56]—the closer to 1 is the value of the "dielectric constant" of the remaining implicit medium. Inside the hydrophobic pocket of a protein there are also polar groups surrounding the hydrogen bond, but in contrast to polar solutions, the environment usually does not relax, as the orientations of the polar groups are dictated mostly by the packing of amino acids rather then by their interaction with the hydrogen bond. This means that the electric fields created by the surroundings (polar groups and charges) in the location of the bridging particle may not be consistent with *any* value of dielectric constant. Though clearly the medium influences the hydrogen bond geometry via electric fields, we find that such terms as polarity and/or polarizability are not sufficient to describe the range of effects it can have on the complex.

CONCLUSIONS

We conclude that both cooperative effects within the hydrogen bond chain and a low-polarity protein environment are essential prerequisites for the stabilization of negative charge on the cofactor and thereby for the spectral tuning of the photoreceptor.

An isolated carboxylic acid phenolate H-bond COO···H···(OC) is not a sufficient model for the active site hydrogen bond system in the dark state of the wild-type PYP. The next approximation, a system COO···H···(OC)···H···OC which includes two coupled hydrogen bonds, however, captures a critical phenomenon: cooperative interaction via the phenolic oxygen atom of the cofactor subunit displaces the bridging proton toward the carboxylate group (Figure 7). As a result, the model cofactor subunit behaves toward the carboxylate as would a phenol with much higher intrinsic acidity (lower pK_a value). A third approximation, a model taking into account the hydrogen bond between Tyr42 and Thr50, i.e., COO···H···(OC)···H···(OC)···H···(OC), in which the last proton donor is an aliphatic hydroxyl group shows that formation of such a remote long third hydrogen bond has only little impact on the geometry of the hydrogen bond between the carboxylic group and the cofactor model subunit.

However, every individual H-bond in the chain eventually aides to stabilize the negative charge and reduce the apparent pK_a value of the system as a whole. This effect has not been quantified in the present work, but it has been shown for molecular photoswitches that already a single quasi-symmetric intramolecular H-bond between carboxylic[57] or phenolic[58] residues may reduce the first pK_a of the joined system by more than 2 units relative to the pK_a of the spatially separated moieties.

Our results further indicate that the PYP active site protein environment is preferentially modeled by a low-polarity aprotic medium. In such a medium, charge is best stabilized in extended conjugated systems as the cofactor offers. In polar media, especially in protic polar media such as water, charge is most effectively stabilized by solvation when confined to

https://doi.org/10.1021/acs.jpcb.0c09923
J. Phys. Chem. B XXXX, XXX, XXX−XXX

smaller entities, such as a carboxylic group. Hence, comparison of pK_a values obtained in water of phenolic and carboxylic groups may not reflect the relative proton donating abilities of such groups in an apolar medium.

■ ASSOCIATED CONTENT

Supporting Information

The Supporting Information is available free of charge at https://pubs.acs.org/doi/10.1021/acs.jpcb.0c09923.

Syntheses of the model compounds, all experimental details, and additional tables of spectroscopic data (PDF)

■ AUTHOR INFORMATION

Corresponding Author

Benjamin Koeppe − *J. Heyrovský Institute of Physical Chemistry, 182 23 Prague 8, Czech Republic;* orcid.org/0000-0002-5420-6392; Email: bekay@chemie.fu-berlin.de

Authors

Peter M. Tolstoy − *Institute of Chemistry, St. Petersburg State University, 198504 St. Petersburg, Russia;* orcid.org/0000-0002-8426-3988

Jing Guo − *Department of Radiology, Charité - Universitätsmedizin Berlin, 10117 Berlin, Germany*

Gleb S. Denisov − *Department of Physics, St. Petersburg State University, 198504 St. Petersburg, Russian Federation*

Hans-Heinrich Limbach − *Institut für Chemie und Biochemie, Freie Universität Berlin, 14195 Berlin, Germany;* orcid.org/0000-0002-2084-6359

Complete contact information is available at: https://pubs.acs.org/10.1021/acs.jpcb.0c09923

Funding

H.-H.L.: DFG Li 300/29-1; P.M.T.: RSF 18-13-00050.

Notes

The authors declare no competing financial interest.

■ REFERENCES

(1) Meyer, T. E. Isolation and Characterization of Soluble Cytochromes, Ferredoxins and Other Chromophoric Proteins from the Halophilic Phototrophic Bacterium Ectothiorhodospira Halophila. *Biochim. Biophys. Acta, Bioenerg.* **1985**, *806*, 175−183.

(2) Sprenger, W. W.; Hoff, W. D.; Armitage, J. P.; Hellingwerf, K. J. The Eubacterium Ectothiorhodospira Halophila is Negatively Phototactic, with a Wavelength Dependence that Fits the Absorption Spectrum of the Photoactive Yellow Protein. *J. Bacteriol.* **1993**, *175*, 3096−3104.

(3) Meyer, T. E.; Yakali, E.; Cusanovich, M. A.; Tollin, G. Properties of a Water-Soluble, Yellow Protein Isolated from a Halophilic Phototrophic Bacterium that Has Photochemical Activity Analogous to Sensory Rhodopsin. *Biochemistry* **1987**, *26*, 418−423.

(4) Borgstahl, G. E. O.; Williams, D. R.; Getzoff, E. D. 1.4 Å Structure of Photoactive Yellow Protein, a Cytosolic Photoreceptor: Unusual Fold, Active Site, and Chromophore. *Biochemistry* **1995**, *34*, 6278−6287.

(5) Yamaguchi, S.; Kamikubo, H.; Kurihara, K.; Kuroki, R.; Niimura, N.; Shimizu, N.; Yamazaki, Y.; Kataoka, M. Low-barrier Hydrogen Bond in Photoactive Yellow Protein. *Proc. Natl. Acad. Sci. U. S. A.* **2009**, *106*, 440−444.

(6) Brudler, R.; Meyer, T. E.; Genick, U. K.; Devanathan, S.; Woo, T. T.; Millar, D. P.; Gerwert, K.; Cusanovich, M. A.; Tollin, G.; Getzoff, E. D. Coupling of Hydrogen Bonding to Chromophore Conformation and Function in Photoactive Yellow Protein. *Biochemistry* **2000**, *39*, 13478−13486.

(7) Kim, M.; Mathies, R. A.; Hoff, W. D.; Hellingwerf, K. J. Resonance Raman Evidence that the Thioester-linked 4-Hydroxycinnamyl Chromophore of Photoactive Yellow Protein is Deprotonated. *Biochemistry* **1995**, *34*, 12669−12672.

(8) Yoda, M.; Houjou, H.; Inoue, Y.; Sakurai, M. Spectral Tuning of Photoactive Yellow Protein. Theoretical and Experimental Analysis of Medium Effects on the Absorption Spectrum of the Chromophore. *J. Phys. Chem. B* **2001**, *105*, 9887−9895.

(9) Baca, M.; Borgstahl, G. E. O.; Boissinot, M.; Burke, P. M.; Williams, D. R.; Slater, K. A.; Getzoff, E. D. Complete Chemical Structure of Photoactive Yellow Protein: Novel Thioester-Linked 4-Hydroxycinnamyl Chromophore and Photocycle Chemistry. *Biochemistry* **1994**, *33*, 14369−14377.

(10) Oktaviani, N. A.; Pool, T. J.; Yoshimura, Y.; Kamikubo, H.; Scheek, R. M.; Kataoka, M.; Mulder, F. A. A. Active-Site pKa Determination for Photoactive Yellow Protein Rationalizes Slow Ground-State Recovery. *Biophys. J.* **2017**, *112*, 2109−2116.

(11) Oktaviani, N. A.; Pool, T. J.; Kamikubo, H.; Slager, J.; Scheek, R. M.; Kataoka, M.; Mulder, F. A. A. Comprehensive Determination of Protein Tyrosine pK_a Values for Photoactive Yellow Protein Using Indirect ^{13}C NMR Spectroscopy. *Biophys. J.* **2012**, *102*, 579−586.

(12) Dawson, R. M. C.; Elliot, D. C.; Elliot, W. H.; Jones, K. M. *Data for Biochemical Research*; Oxford Science Publications: Oxford, 1986.

(13) Kroon, A. R.; Hoff, W. D.; Fennema, H. P. M.; Gijzen, J.; Koomen, G.-J.; Verhoeven, J. W.; Crielaard, W.; Hellingwerf, K. J. Spectral Tuning, Fluorescence, and Photoactivity in Hybrids of Photoactive Yellow Protein, Reconstituted with Native or Modified Chromophores. *J. Biol. Chem.* **1996**, *271*, 31949−31956.

(14) Genick, U. K.; Devanathan, S.; Meyer, T. E.; Canestrelli, I. L.; Williams, E.; Cusanovich, M. A.; Tollin, G.; Getzoff, E. D. Active Site Mutants Implicate Key Residues for Control of Color and Light Cycle Kinetics of Photoactive Yellow Protein. *Biochemistry* **1997**, *36*, 8−14.

(15) Hendriks, J.; Hoff, W. D.; Crielaard, W.; Hellingwerf, K. J. Protonation/Deprotonation Reactions Triggered by Photoactivation of Photoactive Yellow Protein from Ectothiorhodospira halophila. *J. Biol. Chem.* **1999**, *274*, 17655−17660.

(16) Pinney, M. M.; Natarajan, A.; Yabukarski, F.; Sanchez, D. M.; Liu, F.; Liang, R.; Doukov, T.; Schwans, J. P.; Martinez, T. J.; Herschlag, D. Structural Coupling Throughout the Active Site Hydrogen Bond Networks of Ketosteroid Isomerase and Photoactive Yellow Protein. *J. Am. Chem. Soc.* **2018**, *140*, 9827−9843.

(17) Joshi, C. P.; Otto, H.; Hoersch, D.; Meyer, T. E.; Cusanovich, M. A.; Heyn, M. P. Strong Hydrogen Bond between Glutamic Acid 46 and Chromophore Leads to the Intermediate Spectral Form and Excited State Proton Transfer in the Y42F Mutant of the Photoreceptor Photoactive Yellow Protein. *Biochemistry* **2009**, *48*, 9980−9993.

(18) Graen, T.; Inhester, L.; Clemens, M.; Grubmüller, H.; Groenhof, G. The Low Barrier Hydrogen Bond in the Photoactive Yellow Protein: A Vacuum Artifact Absent in the Crystal and Solution. *J. Am. Chem. Soc.* **2016**, *138*, 16620−16631.

(19) Sharif, S.; Denisov, G. S.; Toney, M. D.; Limbach, H.-H. NMR Studies of Coupled Low- and High-Barrier Hydrogen Bonds in Pyridoxal-5′-phosphate Model Systems in Polar Solution. *J. Am. Chem. Soc.* **2007**, *129*, 6313−6327.

(20) Yoda, M.; Inoue, Y.; Sakurai, M. Effect of Protein Environment on pKa Shifts in the Active Site of Photoactive Yellow Protein. *J. Phys. Chem. B* **2003**, *107*, 14569−14575.

(21) Koeppe, B.; Guo, J.; Tolstoy, P. M.; Denisov, G. S.; Limbach, H.-H. Solvent and H/D Isotope Effects on the Proton Transfer Pathways in Heteroconjugated Hydrogen-Bonded Phenol-Carboxylic Acid Anions Observed by Combined UV-vis and NMR Spectroscopy. *J. Am. Chem. Soc.* **2013**, *135*, 7553−7566.

(22) Taenzler, P. J.; Sadeghian, K.; Ochsenfeld, C. A Dynamic Equilibrium of Three Hydrogen-Bond Conformers Explains the NMR

Spectrum of the Active Site of Photoactive Yellow Protein. *J. Chem. Theory Comput.* **2016**, *12*, 5170−5178.
(23) Hydrolysis of the thioesters by residual water is driven by the precipitation of hydroxycinnamic acid which is almost insoluble in halocarbons.
(24) Koeppe, B.; Tolstoy, P. M.; Limbach, H.-H. Reaction Pathways of Proton Transfer in Hydrogen-Bonded Phenol-Carboxylate Complexes Explored by Combined UV-Vis and NMR Spectroscopy. *J. Am. Chem. Soc.* **2011**, *133*, 7897−7908.
(25) Jencks, W.; Regenstein, J. In *Handbook of Biochemistry and Molecular Biology*; Fasman, G. D., Ed.; CRC Press: Cleveland, OH, 1976; Vol. *1*, pp 305−351.
(26) Smirnov, S. N.; Golubev, N. S.; Denisov, G. S.; Benedict, H.; Schah-Mohammedi, P.; Limbach, H.-H. Hydrogen/Deuterium Isotope Effects on the NMR Chemical Shifts and Geometries of Intermolecular Low-Barrier Hydrogen-Bonded Complexes. *J. Am. Chem. Soc.* **1996**, *118*, 4094−4101.
(27) Limbach, H. H.; Denisov, G. S.; Golubev, N. S. In *Isotope Effects in Chemistry and Biology*; Kohen, A., Limbach, H. H., Eds.; Taylor & Francis: Boca Raton, FL, 2006; pp 193−230.
(28) Tolstoy, P. M.; Schah-Mohammedi, P.; Smirnov, S. N.; Golubev, N. S.; Denisov, G. S.; Limbach, H.-H. Characterization of Fluxional Hydrogen-Bonded Complexes of Acetic Acid and Acetate by NMR: Geometries and Isotope and Solvent Effects. *J. Am. Chem. Soc.* **2004**, *126*, 5621−5634.
(29) Sorgenfrei, N.; Hioe, J.; Greindl, J.; Rothermel, K.; Morana, F.; Lokesh, N.; Gschwind, R. M. NMR Spectroscopic Characterization of Charge Assisted Strong Hydrogen Bonds in Brønsted Acid Catalysis. *J. Am. Chem. Soc.* **2016**, *138*, 16345−16354.
(30) Limbach, H.-H.; Tolstoy, P. M.; Pérez-Hernández, N.; Guo, J.; Shenderovich, I. G.; Denisov, G. S. OHO Hydrogen Bond Geometries and NMR Chemical Shifts: From Equilibrium Structures to Geometric H/D Isotope Effects, with Applications for Water, Protonated Water, and Compressed Ice. *Isr. J. Chem.* **2009**, *49*, 199−216.
(31) Sternberg, U.; Brunner, E. The Influence of Short-Range Geometry on the Chemical Shift of Protons in Hydrogen Bonds. *J. Magn. Reson., Ser. A* **1994**, *108*, 142−150.
(32) Harris, T. K.; Zhao, Q.; Mildvan, A. S. NMR Studies of Strong Hydrogen Bonds in Enzymes and in a Model Compound. *J. Mol. Struct.* **2000**, *552*, 97−109.
(33) Jeffrey, G. A.; Yeon, Y. The Correlation Between Hydrogen-Bond Lengths and Proton Chemical Shifts in Crystals. *Acta Crystallogr., Sect. B: Struct. Sci.* **1986**, *42*, 410−413.
(34) Gu, Z.; Zambrano, R.; McDermott, A. Hydrogen Bonding of Carboxyl Groups in Solid-State Amino Acids and Peptides: Comparison of Carbon Chemical Shielding, Infrared Frequencies, and Structures. *J. Am. Chem. Soc.* **1994**, *116*, 6368−6372.
(35) Schah-Mohammedi, P.; Shenderovich, I. G.; Detering, C.; Limbach, H.-H.; Tolstoy, P. M.; Smirnov, S. N.; Denisov, G. S.; Golubev, N. S. Hydrogen/Deuterium-Isotope Effects on NMR Chemical Shifts and Symmetry of Homoconjugated Hydrogen-Bonded Ions in Polar Solution. *J. Am. Chem. Soc.* **2000**, *122*, 12878−12879.
(36) Tolstoy, P. M.; Guo, J.; Koeppe, B.; Golubev, N. S.; Denisov, G. S.; Smirnov, S. N.; Limbach, H.-H. Geometries and Tautomerism of OHN Hydrogen Bonds in Aprotic Solution Probed by H/D Isotope Effects on ^{13}C NMR Chemical Shifts. *J. Phys. Chem. A* **2010**, *114*, 10775−10782.
(37) Hansen, P. E. In *Tautomerism*; Antonov, L., Ed.; Wiley-VCH: Weinheim, 2013; pp 145−175.
(38) Hansen, P.; Spanget-Larsen, J. NMR and IR Investigations of Strong Intramolecular Hydrogen Bonds. *Molecules* **2017**, *22*, 552.
(39) Perrin, C. L.; Shrinidhi, A.; Burke, K. D. Isotopic-Perturbation NMR Study of Hydrogen-Bond Symmetry in Solution: Temperature Dependence and Comparison of OHO and ODO Hydrogen Bonds. *J. Am. Chem. Soc.* **2019**, *141*, 17278−17286.
(40) Detering, C.; Tolstoy, P. M.; Golubev, N. S.; Denisov, G. S.; Limbach, H. H. Vicinal H/D Isotope Effects in NMR Spectra of Complexes with Coupled Hydrogen Bonds: Phosphoric Acids. *Dokl. Phys. Chem.* **2001**, *379*, 191−193.
(41) Sigala, P. A.; Tsuchida, M. A.; Herschlag, D. Hydrogen Bond Dynamics in the Active Site of Photoactive Yellow Protein. *Proc. Natl. Acad. Sci. U. S. A.* **2009**, *106*, 9232−9237.
(42) Mulloyarova, V. V.; Giba, I. S.; Kostin, M. A.; Denisov, G. S.; Shenderovich, I. G.; Tolstoy, P. M. Cyclic Trimers of Phosphinic Acids in Polar Aprotic Solvent: Symmetry, Chirality and H/D Isotope Effects on NMR Chemical Shifts. *Phys. Chem. Chem. Phys.* **2018**, *20*, 4901−4910.
(43) Mulloyarova, V. V.; Ustimchuk, D. O.; Filarowski, A.; Tolstoy, P. M. H/D Isotope Effects on ^{1}H-NMR Chemical Shifts in Cyclic Heterodimers and Heterotrimers of Phosphinic and Phosphoric Acids. *Molecules* **2020**, *25*, 1907−1923.
(44) Tolstoy, P. M.; Koeppe, B.; Denisov, G. S.; Limbach, H.-H. Combined NMR and UV/Vis Spectroscopy in the Solution State: Study of the Geometries of Strong OHO Hydrogen Bonds of Phenols with Carboxylic Acids. *Angew. Chem., Int. Ed.* **2009**, *48*, 5745−5747.
(45) Siano, D. B.; Metzler, D. E. Shapes of spectral bands of visual pigments. *J. Chem. Phys.* **1969**, *51*, 1856−1861.
(46) For details on the evaluation of relative signal intensities in terms of deuteron fractions and isotope fractionation, see section 2.3.2 of the Supporting Information.
(47) Kreevoy, M. M.; Liang, T. M. Structures and Isotopic Fractionation Factors of Complexes, A1HA2. *J. Am. Chem. Soc.* **1980**, *102*, 3315−3322.
(48) The UV/NMR cuvettes according to ref 44 used for samples in dichloromethane solution offer superior optical quality but are unfortunately not suitable for the gas transfer procedures necessary for the preparation of samples with pressure-liquefied gases as solvents.
(49) That signal's label DH is purposefully *not* referred to here because the label contains a statement that is dependent on the assumption which was made early on and which is presently under scrutiny.
(50) Site-specific fractions are defined as, for example, $x_{\underline{D}LL} = c_{\underline{D}LL}/(c_{\underline{H}LL} + c_{\underline{D}LL})$. See also section 2.3.2 of the Supporting Information.
(51) Because of their nonplanarity, all H-bonded structures in Figure 2 are chiral (except for **2a** if one assumes a symmetric H-bond), but **4b** additionally bears the stereocenter of the *s*-Bu group (prepared from racemic precursors) and thus exists in diasteriomeric forms.
(52) Morgan, S. O.; Lowry, H. H. Dielectric Polarization of Some Pure Organic Compounds in the Dissolved, Liquid, and Solid States. *J. Phys. Chem.* **1930**, *34*, 2385−2432.
(53) Shenderovich, I. G.; Burtsev, A. P.; Denisov, G. S.; Golubev, N. S.; Limbach, H.-H. Influence of the Temperature-dependent Dielectric Constant on the H/D Isotope Effects on the NMR Chemical Shifts and the Hydrogen Bond Geometry of the Collidine-HF Complex in CDF3/CDClF2 Solution. *Magn. Reson. Chem.* **2001**, *39*, S91−S99.
(54) Sigala, P. A.; Ruben, E. A.; Liu, C. W.; Piccoli, P. M. B.; Hohenstein, E. G.; Martínez, T. J.; Schultz, A. J.; Herschlag, D. Determination of Hydrogen Bond Structure in Water versus Aprotic Environments To Test the Relationship Between Length and Stability. *J. Am. Chem. Soc.* **2015**, *137*, 5730−5740.
(55) Li, L.; Li, C.; Zhang, Z.; Alexov, E. On the Dielectric "Constant" of Proteins: Smooth Dielectric Function for Macromolecular Modeling and Its Implementation in DelPhi. *J. Chem. Theory Comput.* **2013**, *9*, 2126−2136.
(56) Pylaeva, S.; Allolio, C.; Koeppe, B.; Denisov, G. S.; Limbach, H.-H.; Sebastiani, D.; Tolstoy, P. M. Proton Transfer in a Short Hydrogen Bond Caused by Solvation Shell Fluctuations: an ab Initio MD and NMR/UV Study of an $(OHO)^-$ Bonded System. *Phys. Chem. Chem. Phys.* **2015**, *17*, 4634−4644.
(57) Massaad, J.; Micheau, J. C.; Coudret, C.; Sanchez, R.; Guirado, G.; Delbaere, S. Gated Photochromism and Acidity Photomodulation of a Diacid Dithienylethene Dye. *Chem. - Eur. J.* **2012**, *18*, 6568−75.
(58) Koeppe, B.; Rühl, S.; Römpp, F. Towards More Effective, Reversible pH Control by Visible Light Alone: A Thioindigo

https://doi.org/10.1021/acs.jpcb.0c09923
J. Phys. Chem. B XXXX, XXX, XXX−XXX

Photoswitch Undergoing a Strong pK_a Modulation by Isomer-Specific Hydrogen Bonding. *ChemPhotoChem.* **2019**, *3*, 71−74.

https://doi.org/10.1021/acs.jpcb.0c09923
J. Phys. Chem. B XXXX, XXX, XXX−XXX